中国激光

一维纳米材料位姿调控与激光连接技术进展

万辉[1]，赵强[1]，于圣韬[2]，栾世奕[2]，桂成群[1*]，周圣军[1,2**]

[1]武汉大学工业科学研究院，湖北 武汉 430072；

[2]武汉大学动力与机械学院，湖北 武汉 430072；

摘要 一维纳米材料在微/纳机电系统、柔性透明导电器件、传感器等领域具有广泛的应用。将一维纳米材料装配至指定位置并以特定姿态与纳观或宏观材料形成连接是纳米结构实现功能化、器件化的关键。当前已有多种对一维纳米材料进行位姿调控的方法，根据这些调控方法的原理，将其分为探针法、自组装和光镊法三类，重点介绍了这三种一维纳米材料位姿调控方法的原理与特点。结合一维纳米材料的位姿调控方法与激光连接过程，详细阐述了激光连接一维纳米材料领域的新进展。

关键词 激光；激光连接；一维纳米材料；位姿操作

中图分类号 TG456.7 **文献标志码** A **doi**：10.3788/CJL202148.0802003

1 引 言

一维纳米材料通常是指直径为 1～100 nm、长度方向没有限制的纳米管或纳米线。一维纳米材料具有独特的力学、电学、热学、光学等特性，在微/纳机电系统[1-4]、传感器[5-10]、柔性透明导电器件[11-13]等领域具有广阔的应用。与零维纳米材料或二维纳米薄膜相比，一维纳米材料具有较大的长径比。采用一维纳米材料构建纳米结构或器件时，不仅需要考虑一维纳米材料的位置，而且需要考虑其姿态（或偏转角度）。例如，采用 InP、ZnO 等纳米线制备偏振光探测器时，需要将纳米线沉积在电极对上，且纳米线要以平行于两个电极连线的姿态与电极相连接，使偏振光探测器输出的电信号与输入光的偏振角度相对应，否则无法精确测量入射光的偏振角。因此，将一维纳米材料装配至指定位置并以特定姿态与纳观或宏观尺度材料互连是纳米结构实现功能化、器件化的关键。

尽管一维纳米材料具有广阔的应用前景，但是对其位置和姿态进行精确调控并将其与其他材料形成可靠的纳米尺度互连面临着巨大的挑战。一方面，纳米材料的小尺寸使其难以被精确定位，适用于常规材料的操作方法，如机械夹持等方法，容易对纳米材料造成损伤；另一方面，纳米材料比表面积大、表面能高，将能量精准地投放到纳米材料的连接部位而不影响纳米材料的非连接部位是制备高性能纳米接头的关键。目前，已有多种对一维纳米材料位姿进行精确调控的方法。根据这些纳米操作方法的原理，可将其分为探针法、自组装和光镊法三类。针对一维纳米材料的连接问题，已有机械压[14-16]、热退火[17-18]、化学处理[19-20]、冷焊[21-22]、激光诱导[23-25]等多种纳连接方法。激光诱导纳米连接技术是利用激光辐照纳米材料，在纳米材料上激发局部表面等离激元共振，从而在一维纳米材料的两端和纳米材料间的缝隙处产生局部热效应[26-27]。通过精确调控激光对纳米材料的辐照强度，可以使纳米材料的互连位置受热，产生相变微熔效果，然后通过冷凝将纳米材料与纳观或宏观材料连接。当材料尺寸减小至纳米尺度后，材料的比表面积显著增大，表面能升高，纳米材料的熔点显著降低[28-29]。这种特性导致纳米材料在热作用下很容易被氧化，从而降低纳米材料的电学性能。与热压、热退火等纳连接技术相比，激光诱导纳米连接技术具有局部加热特性，在实现纳米尺度互连的同时，对纳米材料非连接部位的影响

收稿日期：2020-12-01；**修回日期**：2020-12-30；**录用日期**：2021-02-23

基金项目：国家重点研发计划（2017YFB1104900）、国家自然科学基金（52075394，51675386，51775387）

*E-mail：cheng.gui.2000@gmail.com；**E-mail：zhousj@whu.edu.cn

较小，是一种高效率、低损伤的连接方式[10]。本文结合一维纳米材料的位姿调控技术与激光连接一维纳米材料过程，重点阐述了探针法、自组装和光镊法三类一维纳米材料位姿调控方法的原理、应用及优缺点，详细介绍了激光连接一维纳米材料领域的新进展，以期为后续纳米连接技术与装备的发展提供参考。

2　基于探针法的激光连接技术进展

探针法利用探针拨动纳米材料，进而对一维纳米材料的位置和姿态进行高精度调控。由于一维纳米材料的尺寸非常小，探针法采用的探针针尖一般为纳米尺度。此外，为了对一维纳米材料的位置进行标定，探针法还需借助高分辨率显微镜。探针法使用的显微镜包括光学显微镜、原子力显微镜和扫描电镜等，使用的探针包括纳米光纤探针、原子力显微镜探针、纳米钨针等。

图 1(a)显示了采用纳米光纤探针对纳米线位置和姿态进行调控的光学系统结构图[30-34]，其中 PL1 和 PL2 是偏振器，HWP 是半波片，BS 是分光片，PBS 是薄膜分束器，MO 是显微镜物镜。该系统主要包含三部分，分别是光学显微镜，探针和激光。光学显微镜由电荷耦合器件(Charge Coupled Device，CCD)和 100×镜组合而成，用来对一维纳米材料的位置进行标定。图 1(b)显示了该系统使用的纳米光纤探针的扫描电镜图。该纳米光纤探针由 SMF-28 光纤经熔融拉伸后制备而成。图 1(c)显示了在该显微镜下直径为 270～370 nm 的 Au 纳米线。该系统采用的激光波长为 532 nm，激光器产生的激光束经过物镜聚焦后，光斑直径被缩小至 500 nm 左右，可以将激光精确投射至纳米材料的连接位置。该系统工作时，首先通过光学显微镜对一维纳米材料的位置进行标定；然后将探针针尖移至物镜下方，在光学显微镜和三维移动平台的辅助下，对纳米线的位置和姿态进行调控；最后将激光输入到纳米材料的连接位置，实现纳米尺度互连。

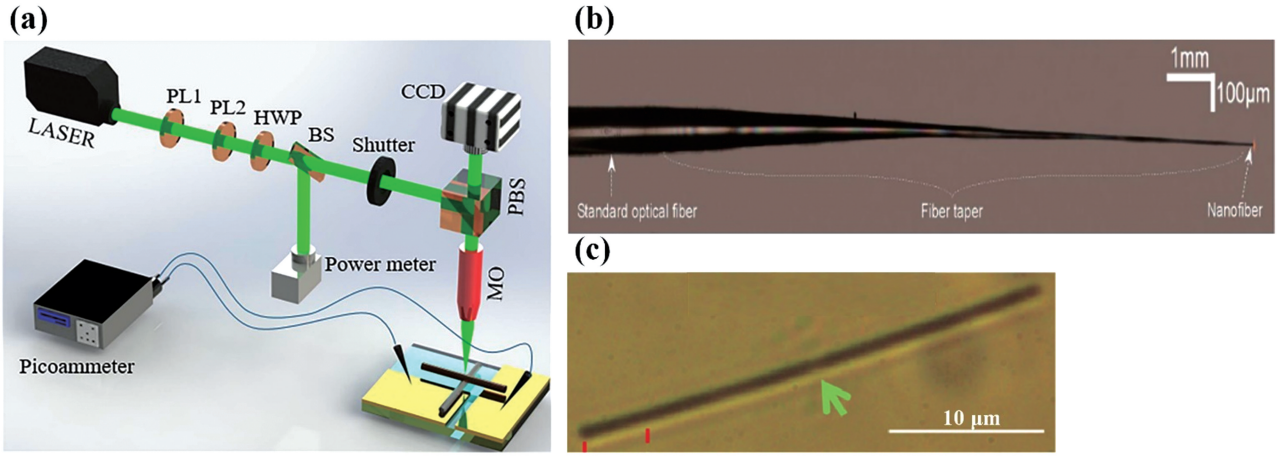

图 1　采用光学显微镜辅助的探针系统。(a)采用光学显微镜辅助纳米操作系统的原理图[30]；(b)光纤熔融拉伸制备的光纤探针[35]；(c)直径为 270 ～370 nm 的 Au 纳米线的光学图像[33]

Fig. 1　Probe system assisted using optical microscope. (a) Principle diagram of nano-operating system assisted using optical microscope[30]; (b) fiber probe prepared by melting and stretching fiber[35]; (c) optical microscope of Au nanowire with diameter of 270–370 nm[33]

浙江大学的 Li 等[32]采用图 1 所示的探针系统，使两根 Ag 纳米线呈 90°交叉姿态，然后利用激光辐照下方的 Ag 纳米线，使下方的 Ag 纳米线熔化收缩并包裹住上方的 Ag 纳米线，产生钎焊效果，如图 2(a)、(b)所示。图 2(c)、(d)显示了两根末端搭接呈“V”型的 Ag 纳米线。激光辐照两根 Ag 纳米线的搭接处，使两根 Ag 纳米线在搭接处熔化，在冷凝后形成互连结构。利用该探针系统，浙江大学的 Ghosh 等[30]将 Ag 纳米线以垂直于 ZnO 纳米线的姿态放置在 ZnO 纳米线的上方，利用激光辐照 Ag 纳米线一端，Ag 纳米线熔化后包裹住 ZnO 纳米线，制备出金属-半导体异质纳米接头，如图 2(e)所示。图 2(f)显示了激光辐照 Ag 纳米线后的温度分布，仿真采用的激光输入功率为 30 mW。图 2(g)显示了 ZnO 纳米线与 Au 电极连接后的形貌图。ZnO 纳米线与 Au 电极形成连接后，测量得到的 ZnO-Au 异质纳米接头的电流-电压(I-V)曲线如图 2(h)所示。ZnO 纳米线与 Au 电极连接前后的 I-V 曲线表明，ZnO 纳米线与 Au 电极形成了肖特基接触[30]。

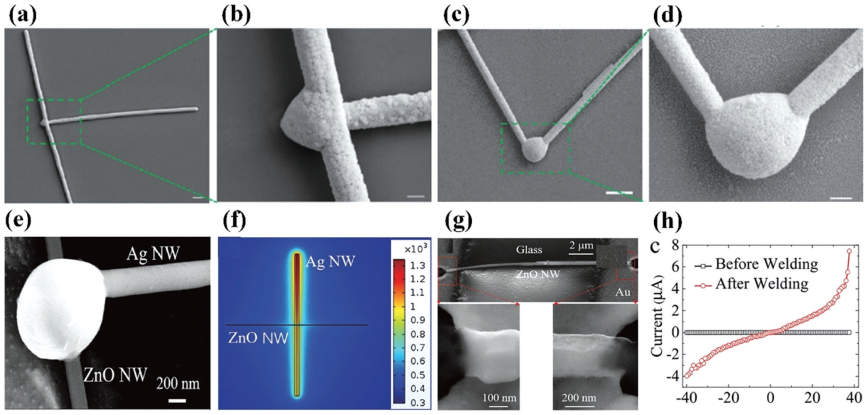

图 2　激光制备纳米接头。(a)(b)利用两根垂直交叉的 Ag 纳米线制备的“T”型钎焊接头[32]；(c)(d)利用两根末端接触的 Ag 纳米线制备的“V”型纳米接头，比例尺为 1 μm[32]；(e)Ag 纳米线在 ZnO 纳米线上方垂直交叉，激光辐照后 Ag 纳米线包裹 ZnO 纳米线[30]；(f)采用功率为 30 mW 的连续波激光辐照 ZnO 上方的银纳米线一端，Comsol 仿真计算出的 Ag 和 ZnO 纳米线的温度分布[30]；(g)激光辐照后，ZnO 纳米线与 Au 电极连接后的形貌图[30]；(h)ZnO 纳米线和 Au 电极形成连接前后的电学特性[30]

Fig. 2　Nano-joints prepared with laser. (a)(b) Scanning electron microscope (SEM) image of T-shaped brazing joint prepared by using two perpendicularly crossed Ag nanowires[32]; (c)(d) V-shaped nano-joint prepared by using two crossed Ag nanowires with scale of 1 μm[32]; (e) Ag nanowires vertically crossed above ZnO nanowires, and Ag nanowires wrapped ZnO nanowires after laser irradiation [30]; (f) temperature distributions of Ag and ZnO nanowires simulated by COMSOL when 30 mW laser is focused at one end of Ag nanowires above ZnO[30]; (g) morphology of ZnO nanowires connected with Au electrode after laser irradiation[30]; (h) electrical characteristics of ZnO nanowires and Au electrodes before and after forming connection[30]

采用光学显微镜辅助探针系统的主要优点是结构简单、价格低廉、操作简单，可以将激光直接耦合到光学显微镜系统中，实现原位纳米连接。此外，还可以直接将激光耦合进光纤探针中，将激光传导至纳米光纤探针的针尖处，而后将探针深入纳米材料的连接位置，实现高精度的点焊[35]。该系统的主要缺点是光学显微镜的分辨率较低，对尺寸小于 100 nm 材料的定位精度差。此外，随着物镜分辨率的提高，物镜的有效焦深和工作距离逐渐减小，导致探针操作空间急剧减小。这些因素限制了该系统在纳连接领域的应用。

为了提高纳米操作精度，必须采用更高精度的显微镜辅助探针进行纳米操作。崔健磊等[36-37]采用原子力显微镜(Atomic Force Microscopy，AFM)探针，对碳纳米管的位置和姿态进行高精度调控，然后利用激光在 AFM 探针针尖处激发近场增强效应[38-40]，利用近场增强效应加热钎料，连接碳纳米管。图 3(a)显示了 AFM 探针调控纳米材料位姿的工作流程图。该系统调控一维纳米材料位姿的过程分为 5 个步骤：第一步，通过原子力显微镜的轻敲模式获取纳米材料的位置；第二步，将 AFM 的工作模式保持在轻敲模式，将 AFM 的探针移动至纳米材料前；第三步，将 AFM 的工作模式切换为接触模式，使 AFM 探针作向量式移动，推动纳米材料，进而调控一维纳米材料的位置；第四步，多次重复步骤三，对一维纳米材料的位置和姿态进行精确调控；第五步，切换原子力显微镜的工作模式，移出原子力显微镜探针，完成对碳纳米管的位姿调控。该系统采用 CSPM5500 系列的 AFM 探针操作系统，在 XY 平面内的操作精度可达 0.2 nm。图 3(b)显示了 AFM 探针利用近场增强效应连接碳纳米管的原理图。通过 AFM 探针精确调控碳纳米管的位姿后，利用 AFM 探针蘸取钎料并精确投放在碳纳米管的连接位置，然后利用激光辐照 AFM 探针针尖以激发近场增强效应加热钎料，实现碳纳米管的互连。图 3(c)是该系统采用的 AFM 探针的 SEM 图。图 3(e)、(f)分别显示了碳纳米管连接前后的形貌图，实验采用的激光强度为 40 mW，辐照时间为 3 min，激光加热点位于两根碳纳米管轴向互连中心处。

采用 AFM 探针的优点是，纳米操作精度高，且该系统可通过近场增强效应连接一维纳米材料。该系统的缺点在于，原子力显微镜的成像效率和纳米操作效率相对较低。当前，已有其他高精度探针系

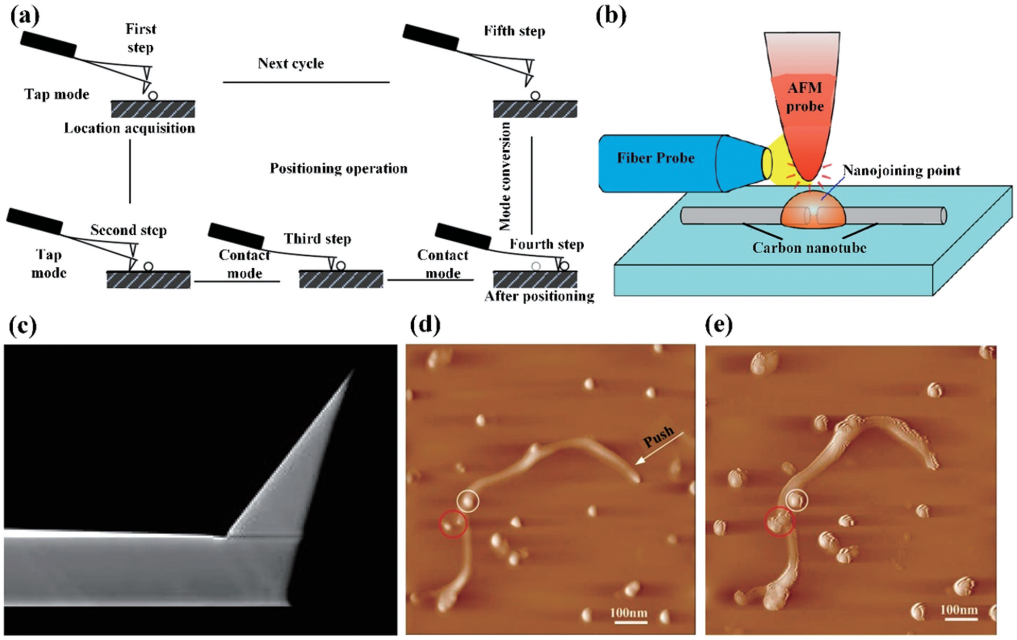

图 3　原子力显微镜辅助的探针系统[37]。(a)AFM 探针系统连接碳纳米管的工作流程图;(b)激光在 AFM 探针针尖激发近场增强效应进而连接两根碳纳米管的原理图;(c)AFM 探针的扫描电镜图;碳纳米管(d)连接前和(e)连接后的 AFM 图

Fig. 3　Probe system assisted by atomic force microscope[37]. (a) Flow chart of AFM probe system connecting carbon nanotubes; (b) principle diagram for nanojoining two carbon nanotubes by using near-field enhancement effect excited at AFM probe tip by laser; (c) SEM image of AFM probe; AFM images (d) before and (e) after nanojoining of carbon nanotubes

统的报道,如透射电子显微镜(Transmission Electron Microscope,TEM)辅助的探针系统。图 4 显示了在 TEM 下利用纳米钨针调控的碳纳米管位姿的形貌图[41]。利用该系统可以清晰地看到碳纳米管连接前后的位姿和形貌变化。该探针系统的工作原理与光学显微镜或 AFM 辅助探针系统的工作原理相似,都是通过探针拨动纳米材料,进而调控一维纳米材料的位置和姿态。

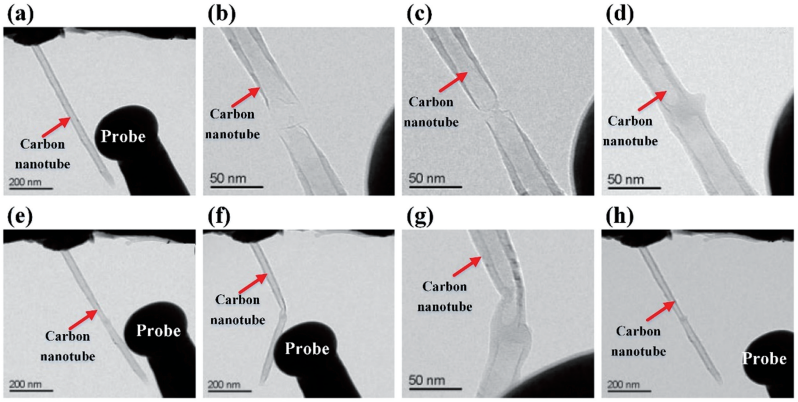

图 4　TEM 辅助的探针系统[41]。(a)碳纳米管连接到 Pt 电极上的形貌图;(b)碳纳米管破裂后的形貌图;(c)破裂后的两根碳纳米管端部接触时的形貌;(d)采用电子束诱导沉积方法制备的碳纳米管-碳纳米管接头;(e)图 4(d)中互连后的碳纳米管形貌图;(f)利用探针对碳纳米管施加垂直轴向的压力测试碳纳米管接头性能;(g)图 4(f)中碳纳米管弯曲位置的放大图像;(h)移开探针后碳纳米管的形貌图

Fig. 4　Probe system assisted by TEM[41]. (a) Morphology of carbon nanotube connected with Pt electrode; (b) morphology of carbon nanotubes after cracking; (c) morphology of two end-contacted carbon nanotubes after cracking; (d) carbon nanotube-carbon nanotube joint prepared by using electron beam induced deposition method; (e) morphology of carbon nanotube after joint in Fig. 4 (d); (f) carbon nanotube joint performance tested by applying vertical axial pressure to carbon nanotubes with probe; (g) enlarged image of bending position of carbon nanotube in Fig. 4 (f); (h) morphology of carbon nanotube after removing probe

基于探针的纳米连接技术是当前研究最广泛的纳米连接技术之一。采用探针的纳米操作设备主要有三大优点：一，探针系统可以实现高精度的纳米操作；二，将激光设备与显微镜结合，可以将能量精准地投射在一维纳米材料的连接部位，实现低损伤、高精度的纳米互连；三，采用探针技术可以对纳米接头的电学、力学等性能进行测试，实现纳米操作、纳米连接、纳米测试一体化。探针技术的主要缺点是只能对单根一维纳米材料进行位姿调控，导致纳米操作效率较低。

3　基于自组装的激光连接技术进展

将批量的一维纳米材料以特定位姿连接后，利用大量纳米功能单元形成纳米功能器件是一维纳米材料实现器件化的关键技术之一。纳米材料的自组装技术为批量纳米操作提供了一种思路[42-43]。纳米材料的自组装是指纳米材料自发形成有序结构的一种技术[44]。利用纳米材料的自组装技术，可以将大量一维纳米材料进行有序排列。根据纳米材料的自组装原理可将其分为三类：一，纳米材料在溶液中受到引力或斥力，在动态平衡下实现自组装[45-48]；二，纳米材料借助于液-气或固-液等界面通过 LB（Langmuir-Blodgett）技术实现自组装[49-50]；三，在外加场（包括电场、磁场、光场等）的作用下[51-54]，纳米材料产生极化现象，在梯度场作用下，极化后的纳米材料会产生定向移动，且溶液与介电纳米材料的相对介电常数能够决定其运动方向，进而实现一维纳米材料的自组装。与前两种自组装技术相比，通过外加场可以快速实现一维纳米材料的位姿调控过程，这种自组装方法在微/纳机电系统制造领域具有独特优势。

图 5(a)显示了碳纳米管在非均匀电场作用下定向运动的原理图。在电场作用下，碳纳米管产生极化现象。在非均匀电场的作用下，极化后的碳纳米管将沿着电场梯度方向运动。上海交通大学的宋晓辉[55]在 Au 电极上对碳纳米管悬浮液进行介电

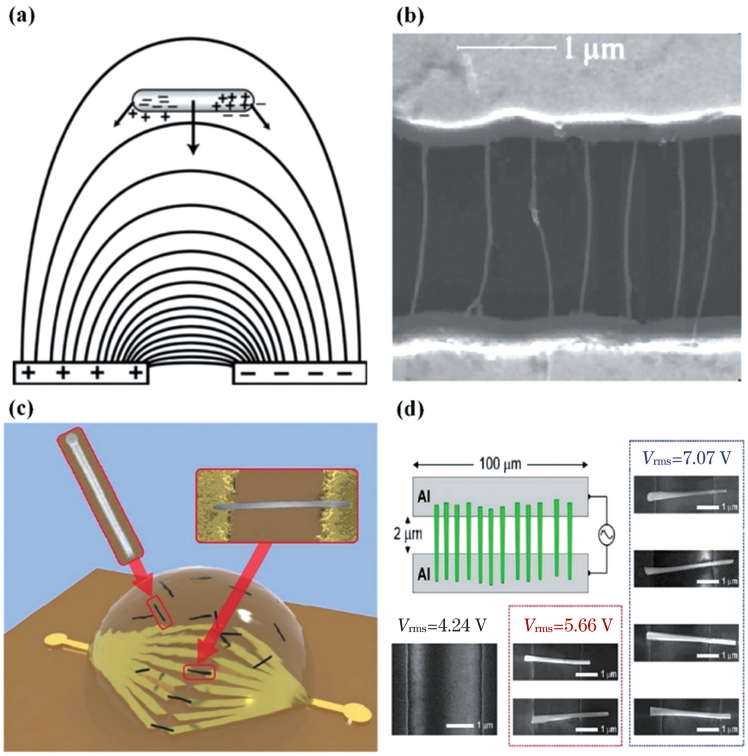

图 5　介电电泳法组装的一维纳米材料。(a)原理图[55]；(b)采用介电电泳法将碳纳米管装配到 Au 电极对上[55]；(c) 在图案化电极衬底上对纳米线溶液进行介电电泳操作的 3D 示意图[53]；(d)在不同的 V_{rms} 和电极几何图式下进行的介电电泳实验的 SEM 图像[53]

Fig. 5　One-dimensional nanomaterials assembled by dielectrophoresis method. (a) Principle diagram[55]; (b) carbon nanotubes deposited onto Au electrodes by dielectrophoresis method[55]; (c) 3D schematic of dielectrophoresis process during drop-casting of carbon nanotube solution over substrate with pre-patterned electrodes[53]; (d) SEM images of dielectrophoresis experiments carried out with different V_{rms} and electrode geometries[53]

电泳操作后，碳纳米管沉积在电极对之间，如图 5(b)所示。施加的交流电电压为 3 V，频率为 3 MHz，电泳时间为 45 s。马德里大学的 Singh 等[53]通过介电电泳制备了基于 GaAs 纳米线的光电探测器。图 5(c)显示了对纳米线分散液进行自组装的原理图。研究者在设计的电极对之间施加频率为 100 kHz 的交流电以捕获 GaAs 纳米线，将直径为 70 ～100 nm 的 GaAs 纳米线装配至电极对上，如图 5(d)所示。实验结果显示，交流电场产生的电泳力是影响自组装效果的关键因素。当施加电压的均方根的平方(V_{rms})为 4.24 V 时，GaAs 纳米线受到的电泳力约为 0.15 nN，此时没有观察到 GaAs 纳米线被捕获；当施加电压的均方根的平方达到 5.66 V 时，GaAs 纳米线受到的电泳力可以克服流体中的阻力，GaAs 纳米线被装配至电极之间。进一步增大 V_{rms} 值至 7.07 V 时，发现 GaAs 纳米线的密度从 0.02 μm^{-1} 增大至 0.08 μm^{-1}[53]。

马德里康普顿斯大学的 González-Rubio 等[56]提出了一种利用低强度飞秒激光组装 Au 纳米棒和利用高强度飞秒激光连接 Au 纳米棒的方法，如图 6(a)所示。该方法采用低通量飞秒激光脉冲辐照 Au 纳米棒悬浮液，使 Au 纳米棒以端对端的方式组装成低聚物，如图 6(b)所示。当激光强度提高至 650 $\mu J/cm^2$ 时，在相邻 Au 纳米棒缝隙处激发局部表面等离激元发生共振，使 Au 纳米棒的末端熔化，在 Au 纳米棒之间形成连接，如图 6(c)所示。首尔国立大学的 Son 等[57]向 Au 纳米棒分散液中添加异丙醇，诱导 Au 纳米棒发生端对端自组装，形成 Au 纳米链，而后以异丙醇为溶剂将 SO_2 涂覆在获得的 Au 纳米链上。图 6(d)、(e)显示了 Au 纳米棒自组装前后的透射电镜图。实验结果显示，添加异丙醇后，Au 纳米棒胶体的消光光谱在大于 1000 nm 的区域内出现了一个新的表面等离激元共振带，如图 6(f)所示。这种实验现象表明，添加异丙醇后 Au 纳米棒自组装形成 Au 纳米链，导致消光光谱带红移。Au 纳米棒自组装形成 Au 纳米链后，利用波长为 1064 nm 的纳秒激光辐照 Au 纳米链，在 Au 纳米棒间的缝隙处激发局部表面等离激元发生共振，选择性地加热 Au 纳米棒的间隙，进而连接 Au 纳米棒。

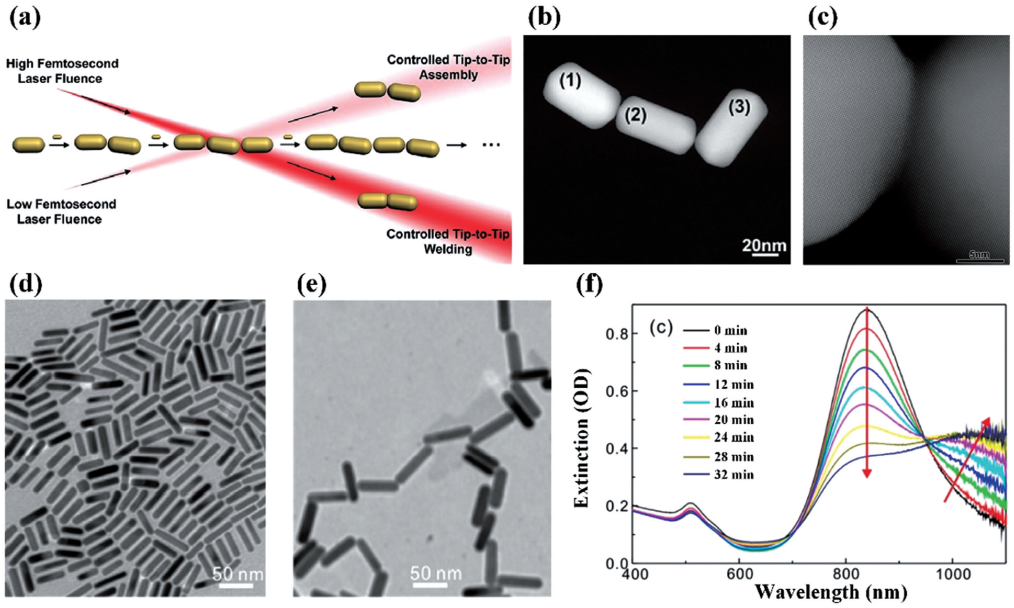

图 6　飞秒激光诱导的自组装。(a)飞秒激光组装并连接 Au 纳米棒的原理图[56]；(b)在强度为 130 $\mu J/cm^2$ 的飞秒激光辐照下 Au 纳米棒的端对端自组装[56]；(c)在强度为 650 $\mu J/cm^2$ 的飞秒激光辐照下 Au 纳米棒末端熔化后互连[56]；Au 纳米棒(d)自组装前和(e)自组装后的 TEM 图[56]；(f)向 0.50 mL 的 Au 纳米棒分散液中加 2.5 mL 异丙醇后，Au 纳米棒胶体的消光光谱随时间的变化曲线[57]

Fig. 6　Self-assembly induced by femtosecond laser. (a) Principle diagram of femtosecond laser self-assembly and joining of Au nanorods[56]; (b) end-to-end self-assembly of Au nanorods under 130 $\mu J/cm^2$ femtosecond laser irradiation [56]; (c) Au nanorods fused and interconnected under 650 $\mu J/cm^2$ femtosecond laser irradiation [56]; TEM images of Au nanorods (d) before and (e) after self-assembly[56]; (f) extinction spectra of Au nanorod colloid versus time after adding 2.5 mL isopropanol to 0.50 mL Au nanorod dispersant[57]

自组装技术可以对批量一维纳米材料进行位姿调控，且操作简单，成本低廉。相比于探针法，自组装技术对一维纳米材料的位姿调控精度相对较低。此外，自组装方法一般在液体环境中进行，可视化效果差。

4　基于光镊的激光连接技术进展

光镊又被称为梯度力光阱（Gradient Force Trap），是一种利用高度会聚激光形成的三维势阱，可以用来俘获、操纵微小粒子。由于光子具有动量，光束的总动量随时间的变化在数值上等于物体受到的光学力[58-59]。这种光学力主要包括光束对纳米材料的推力（又被称为散射力或辐射压力）和拉力（也被称为梯度力）。其中，推力主要来自微小粒子对入射光的散射和吸收；拉力主要来自微小粒子对光的折射和聚焦光束对微小粒子的极化作用，聚焦光束形成的梯度势阱会把微小粒子拉向光场的焦点并束缚在焦点附近[60]。

加州大学的 Pauzauskie 等[61]使用单光束光镊捕获 GaN、SnO_2、Si、ZnO、Ag 纳米线。他们将 1064 nm 的红外激光聚焦后制备出单束光光镊。实验结果显示，激光强度为 30～60 mW 时，该光镊可以捕获 GaN、SnO_2、ZnO、Si 纳米线。对这几种纳米线的位置和姿态进行高精度调控后，将激光器的输出功率提高至 1 W，可成功连接 GaN 与 SnO_2 纳米线，如图 7(a)所示。利用光镊技术，以 GaN 和 SnO_2 纳米线为基本单元搭建出了三维纳米结构，如图 7(b)所示。利用该光镊，他们将单根 GaN 纳米线插入到活细胞中，如图 7(c)所示。由于一维纳米材料可以作为波导[62-63]，将纳米线一端插入到活细胞中后，可以将其作为亚波长照明源，这种一维纳米材料位姿调控方法为活细胞内部组织的成像提供了参考。

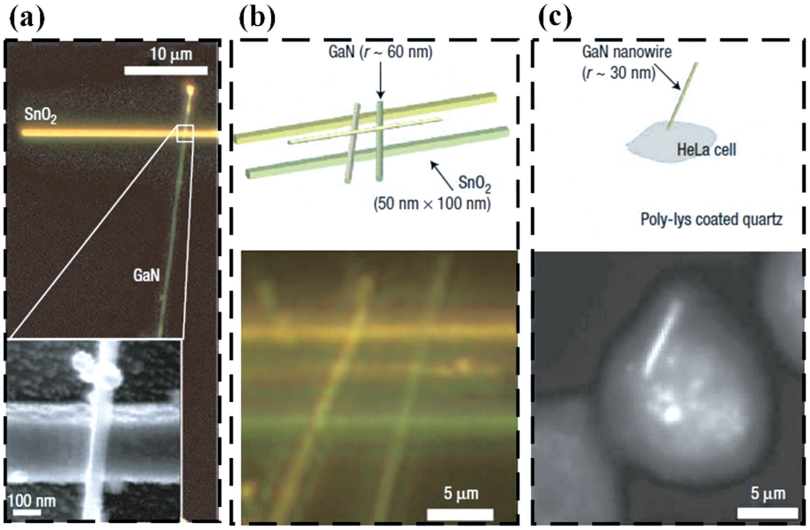

图 7　单束光光镊调控纳米材料位姿[61]。(a)光镊将 GaN 纳米线放置在 SnO_2 纳米线上方，然后采用高强度激光连接 GaN 和 SnO_2 纳米线；(b)光镊通过操控 GaN 和 SnO_2 纳米线，搭建出三维纳米结构；(c)光镊将半径为 30 nm 的 GaN 纳米线插入到活细胞中

Fig. 7　Pose regulation of nanomaterials by single-beam optical tweezer[61]. (a) GaN nanowires placed on top of SnO_2 nanowires by optical tweezer, and then GaN and SnO_2 nanowires connected by high intensity laser; (b) GaN and SnO_2 nanowires manipulated by optical tweezers to form three-dimensional nanostructure; (c) GaN nanowire with radius of 30 nm inserted into living cells by using optical tweezer

尽管单光束光镊可以对一维纳米材料进行高精度的位姿调控，但在实验中还存在可控性差等问题。Pauzauskie 等[61]的研究结果还显示，采用 1064 nm 的红外光光镊捕获 SnO_2 时，有 7% 的 SnO_2 纳米线而出现晃动现象。为了提高光镊对一维纳米材料位姿调控的稳定性，科学家们采用全息光镊对一维纳米材料的位姿进行调控。全息光镊技术由芝加哥大学的 Dufresne 等[64]于 1998 年提出，他们使用衍射光学元件将准直激光束分成多个独立的光束，然后通过聚焦透镜将这些独立光束聚焦成光镊阵列。哈佛大学的 Agarwal 等[65]采用全息光镊对 CdS 纳米线进行高精度位姿调控。图 8(a)、(b)显示了全息光镊捕获 CdS 纳米线的原理图。他们利用液晶空间光调制器将计算机设计的相位全息图压印到激光束的波阵面上，利用该全息图产生实验所需的光镊阵列。当每个光镊的功率控制为 3 mW 时，可对

CdS 纳米线进行平移、旋转等多种复杂的位姿调控，如图 8(c)所示。当单个光镊的功率控制为 0.1～1 W 时，可对 CdS 纳米线进行切割、连接等多种操作，如图 8(d)所示。

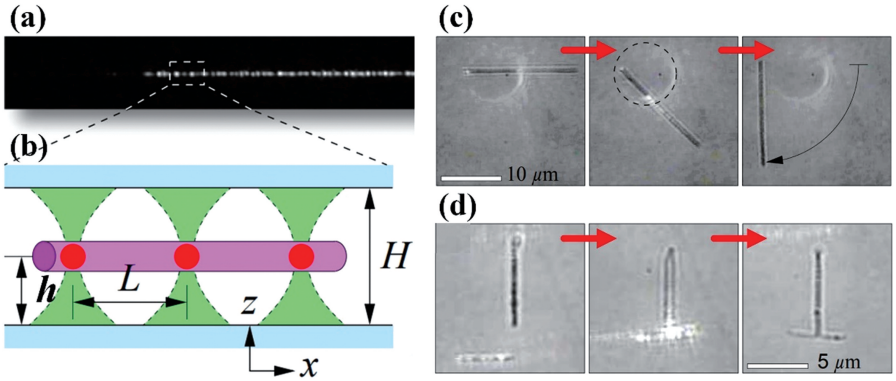

图 8　全息光镊调控一维纳米材料位姿[65]。(a)光镊阵列操作 CdS 纳米线的暗场光学显微镜图；(b)光镊阵列操作 CdS 纳米线的工作原理图；(c)全息光镊旋转 CdS 纳米线；(d)全息光镊移动 CdS 纳米线，并连接两根 CdS 纳米线，形成 T 型纳米接头

Fig. 8　Pose regulation of one-dimensional nanomaterials by holographic optical tweezer[65]. (a) Dark-field optical microscopy of CdS nanowires operated by optical tweezer array; (b) principle diagram of CdS nanowires regulated by optical tweezer array; (c) CdS nanowires rotated by holographic optical tweezers; (d) CdS nanowires moved and two CdS nanowires connected by holographic optical tweezers to form T-shaped nano-joint

光镊能够捕获微小粒子的前提是被捕获粒子受到的梯度力可以克服其受到的散射力，否则激光将对微小粒子产生推力[66-67]。对于宽禁带半导体材料，红外波段的激光可以透过一维纳米材料，此时一维纳米材料受到的散射力较小。对于导电性好的金属纳米材料，其受到的散射力则会显著增加，此时一维纳米材料受到的梯度力难以克服散射力。武汉大学 Wan 等[68]的研究结果显示，对于直径为 50 nm 的 Ag 纳米线，当激光强度达到 3×10^{12} W/m^2 时，Ag 纳米线受到的最大散射力可达到其自身重力的 10^5 倍，从而导致 Ag 纳米线被激光击飞。采用光镊对金属纳米材料进行高精度的位姿调控是一个难点。华盛顿大学的 Crane 等[69]报道了一种采用光镊连接锗纳米线的方法。他们首先在锗纳米线的一端沉积铋纳米球，使带有铋纳米球的锗纳米线可以垂直悬浮在有机溶剂中。采用光镊捕获纳米线时，纳米线的端面而不是侧面被激光辐照，从而显著减小锗纳米线受到的散射力。利用这种方法，光镊对锗纳米线的梯度力可以克服散射力，从而捕获锗纳米线，并在锗纳米线之间形成连接，如图 9(b)所示。南开大学的 Zhang 等[70]采用表面等离激元光镊对 Au 纳米线的位置和姿态进行调控，如图 9(c)所示。他们在玻璃衬底上沉积了一层 45 nm 厚的金薄膜，然后将 754 nm 的线偏振激光经物镜聚焦后投射到金薄膜上，在金薄膜上激发等离子体光镊。利用动态的线偏振激光，他们在平滑的金薄膜上对 Au 纳米线的位置和姿态进行调控，如图 9(d)所示。利用表面等离激元光镊，他们实现了金属纳米材料[70-72]和半导体纳米线[73]的位姿调控。

光镊系统同时具有光学成像功能、高精度纳米操作功能(光源处于低输出功率状态)和激光连接功能(光源处于高输出功率状态)。相比于探针和自组装技术，光镊可对一维纳米材料进行更复杂的二维乃至三维纳米操作，特别适用于构造复杂的纳米结构与器件。光镊技术的缺点是需要在液体环境中工作。

5　总结与展望

重点介绍了一维纳米材料的位姿调控技术与激光连接技术的进展，特别是对一维纳米材料的位置和姿态进行精确调控后，利用激光连接一维纳米材料，从而形成复杂的纳米功能结构。探针技术是目前较为成熟的纳米操作技术，利用探针不仅可以对一维纳米材料的位置和姿态进行高精度调控，还可以使用探针对制备的纳米结构进行电学、力学和可靠性等测试，然而探针技术一般只能对单根纳米材料进行位姿调控，纳米操作效率较低。自组装技术在一维纳米材料的批量操作领域具有独特优势，常用的介电电泳方法需要在特定的电极结构下进行，且对一维纳米材料的位姿调控精度相对较低。光镊技术具有较高的纳米操作精度，可以利用同一个激光源实现纳米操作和激光连接，但是需要在溶液中

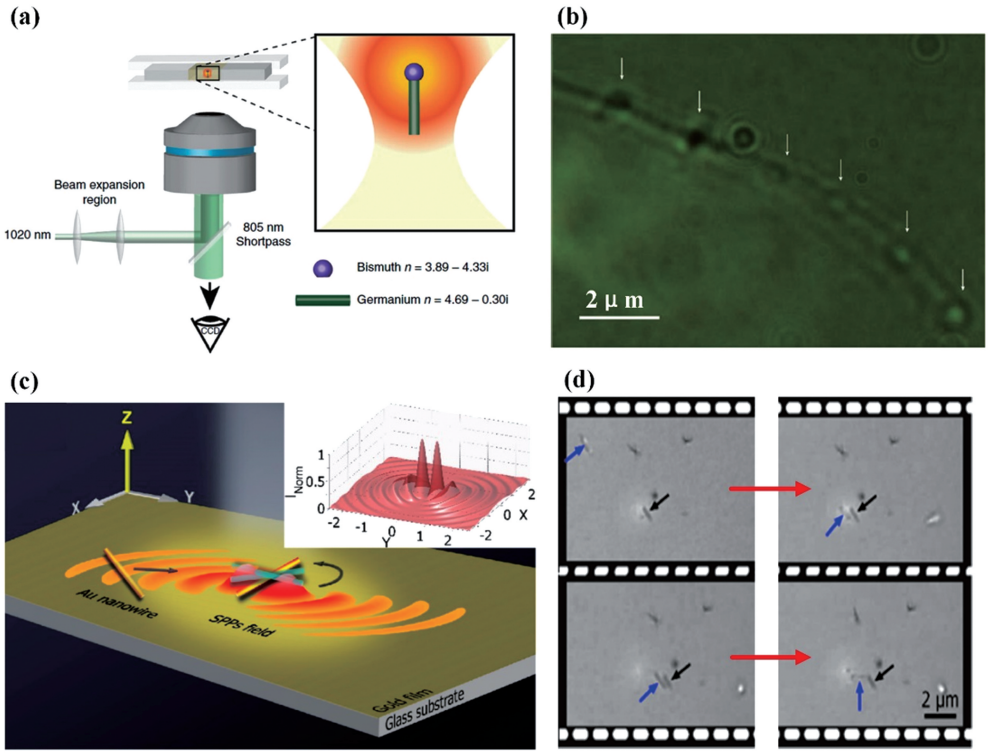

图 9　光镊调控金属纳米线位姿。(a)光镊捕获悬浮在有机溶剂中带有铋纳米球的锗纳米线的原理图[68]；(b)图 9(a)中的锗纳米线连接后的光学显微镜图[68]；(c)采用线偏振激光激发的表面等离激元光镊调控金属纳米线位置和姿态的示意图[70]；(d)两根分离的金纳米线的捕获和组装的连续图像[70]

Fig. 9　Optical tweezer based pose regulation of metal nanowires. (a) Principle diagram of optical tweezer based trapping of germanium nanowires with bismuth nanospheres suspended in organic solvent[68]; (b) optical micrograph of joined germanium nanowires in Fig. 9 (a)[68]; (c) schematic of position and pose regulation by linearly polarized laser excited surface plasmonic tweezer[70]; (d) successive images of trapping and assembly of two separated Au nanowires[70]

进行，对工作环境有较高的要求。提高自组装和光镊技术与现有微电子工艺的兼容性是未来研究的重点。基于上述研究结果，我们认为多技术融合是未来纳米连接领域的发展趋势。例如，激光直写组装技术融合了光镊、自组装和激光直写等技术，可直接组装二维、三维微/纳米机电系统[28]。此外，纳米操作技术正在与激光连接技术、显微技术、纳米测试技术融合，在同一个系统下实现纳米观测、纳米操作、纳米连接以及纳米接头性能测试。这种多功能的纳米连接技术与装备将进一步推动纳米科技的发展与应用，推动多学科交叉，产生更多的创新应用。

参　考　文　献

[1] Qi Y, Zhang T, Jing C Y, et al. Nanocrystal facet modulation to enhance transferrin binding and cellular delivery[J]. Nature Communications, 2020, 11: 1262.

[2] Lin L C, Huo J P, Peng P, et al. Contact engineering of single core/shell SiC/SiO_2 nanowire memory unit with high current tolerance using focused femtosecond laser irradiation[J]. Nanoscale, 2020, 12(9): 5618-5626.

[3] Yu G, Li J C, Wen P J, et al. Research progress on semiconductor micro/nanowire lasers[J]. Chinese Journal of Lasers, 2020, 47(7): 0701011.
于果, 李俊超, 温培钧, 等. 半导体微纳米线激光器研究进展[J]. 中国激光, 2020, 47(7): 0701011.

[4] Xiao Y, Shen D, Zou G, et al. Self-powered, flexible and remote-controlled breath monitor based on TiO_2 nanowire networks[J]. Nanotechnology, 2019, 30(32): 325503.

[5] Zhou H, Song Z N, Grice C R, et al. Self-powered $CsPbBr_3$ nanowire photodetector with a vertical structure[J]. Nano Energy, 2018, 53: 880-886.

[6] Zhao Z J, Ko J, Ahn J, et al. 3D layer-by-layer Pd-containing nanocomposite platforms for enhancing the performance of hydrogen sensors[J]. ACS Sensors, 2020, 5(8): 2367-2377.

[7] Imani S, Bandodkar A J, Mohan A M, et al. A wearable chemical-electrophysiological hybrid biosensing system for real-time health and fitness monitoring[J]. Nature Communications, 2016, 7:

11650.

[8] Han W X, He H X, Zhang L L, et al. A self-powered wearable noninvasive electronic-skin for perspiration analysis based on piezo-biosensing unit matrix of enzyme/ZnO nanoarrays[J]. ACS Applied Materials & Interfaces, 2017, 9(35): 29526-29537.

[9] Economou A, Kokkinos C, Prodromidis M. Flexible plastic, paper and textile lab-on-a chip platforms for electrochemical biosensing[J]. Lab on a Chip, 2018, 18(13): 1812-1830.

[10] Lee H B, Jin W Y, Ovhal M M, et al. Flexible transparent conducting electrodes based on metal meshes for organic optoelectronic device applications: a review[J]. Journal of Materials Chemistry C, 2019, 7(5): 1087-1110.

[11] Liang X W, Zhao T, Zhu P L, et al. Room-temperature nanowelding of a silver nanowire network triggered by hydrogen chloride vapor for flexible transparent conductive films[J]. ACS Applied Materials & Interfaces, 2017, 9(46): 40857-40867.

[12] Chen W, Liu L X, Zhang H B, et al. Flexible, transparent, and conductive $Ti_3C_2T_x$ MXene-silver nanowire films with smart acoustic sensitivity for high-performance electromagnetic interference shielding[J]. ACS Nano, 2020, 14(12): 16643-16653.

[13] Zhou B, Su M J, Yang D Z, et al. Flexible MXene/silver nanowire-based transparent conductive film with electromagnetic interference shielding and electro-photo-thermal performance[J]. ACS Applied Materials & Interfaces, 2020, 12(36): 40859-40869.

[14] Peng P, Guo W, Zhu Y, et al. Nanoscale wire bonding of individual Ag nanowires on Au substrate at room temperature[J]. Nano-Micro Letters, 2017, 9(3): 1-6.

[15] Jung J Y, Qaiser N, Feng G, et al. Size-dependent hardness of five-fold twin structured Ag nanowires[J]. Physical Chemistry Chemical Physics, 2017, 19(2): 1311-1319.

[16] Hwang B, Shin H A S, Kim T, et al. Highly reliable Ag nanowire flexible transparent electrode with mechanically welded junctions[J]. Small, 2014, 10(16): 3397-3404.

[17] Chen D, Liang J J, Liu C, et al. Thermally stable silver nanowire-polyimide transparent electrode based on atomic layer deposition of zinc oxide on silver nanowires[J]. Advanced Functional Materials, 2015, 25(48): 7512-7520.

[18] Langley D P, Lagrange M, Giusti G, et al. Metallic nanowire networks: effects of thermal annealing on electrical resistance[J]. Nanoscale, 2014, 6(22): 13535-13543.

[19] Lu H F, Zhang D, Cheng J Q, et al. Locally welded silver nano-network transparent electrodes with high operational stability by a simple alcohol-based chemical approach[J]. Advanced Functional Materials, 2015, 25(27): 4211-4218.

[20] Ge Y J, Duan X D, Zhang M, et al. Direct room temperature welding and chemical protection of silver nanowire thin films for high performance transparent conductors[J]. Journal of the American Chemical Society, 2018, 140(1): 193-199.

[21] Pereira Z S, da Silva E Z. Cold welding of gold and silver nanowires: a molecular dynamics study[J]. The Journal of Physical Chemistry C, 2011, 115(46): 22870-22876.

[22] Hu A, Peng P, Alarifi H, et al. Femtosecond laser welded nanostructures and plasmonic devices[J]. Journal of Laser Applications, 2012, 24(4): 042001.

[23] Ming X, Shuo Z, Daozhi S, et al. Laser-induced joining of nanoscale materials: processing, properties, and applications[J]. Nanotoday, 2020, 35: 100959.

[24] Lee C, Oh Y, Yoon I S, et al. Flash-induced nanowelding of silver nanowire networks for transparent stretchable electrochromic devices[J]. Scientific Reports, 2018, 8(1): 2763.

[25] Hu Y W, Liang C, Sun X Y, et al. Enhancement of the conductivity and uniformity of silver nanowire flexible transparent conductive films by femtosecond laser-induced nanowelding[J]. Nanomaterials, 2019, 9(5): 673.

[26] Liu L, Peng P, Hu A M, et al. Highly localized heat generation by femtosecond laser induced plasmon excitation in Ag nanowires[J]. Applied Physics Letters, 2013, 102(7): 073107.

[27] Garnett E C, Cai W, Cha J J, et al. Self-limited plasmonic welding of silver nanowire junctions[J]. Nature Materials, 2012, 11(3): 241-249.

[28] Long J, Jiao B, Fan X, et al. Femtosecond laser assembly of one-dimensional nanomaterials and their application[J]. Chinese Journal of Lasers, 2020, 48(2): 0202017.
龙婧, 焦玢璋, 范旭浩等. 飞秒激光组装一维纳米材料及其应用[J]. 中国激光, 2020, 48(2): 0202017.

[29] Zhang S, Chen L. Size effects on melting point based on surface energy and coordination number[J]. Emerging Materials Research, 2019, 8(4): 618-622.

[30] Ghosh P, Lu J S, Chen Z Y, et al. Photothermal-induced nanowelding of metal-semiconductor heterojunction in integrated nanowire units[J].

Advanced Electronic Materials, 2018, 4(5): 1700614.

[31] Zhou L N, Lu J S, Yang H B, et al. Optically controllable nanobreaking of metallic nanowires[J]. Applied Physics Letters, 2017, 110(8): 081101.

[32] Li Q, Liu G P, Yang H B, et al. Optically controlled local nanosoldering of metal nanowires[J]. Applied Physics Letters, 2016, 108(19): 193101.

[33] Dai S W, Li Q, Liu G P, et al. Laser-induced single point nanowelding of silver nanowires[J]. Applied Physics Letters, 2016, 108(12): 121103.

[34] Ghosh P, Lu J S, Luo H, et al. Constructing metal arch nanobridges utilizing a photothermal-induced nanobonding technique[J]. Advanced Electronic Materials, 2019, 5(7): 1800807.

[35] Zhou L N. Light-induced photothermal nanowelding and nanobreaking of metallic nanowires[D]. Hangzhou: Zhejiang University, 2017.
周莉娜. 基于光热效应的金属纳米线焊接与熔断[D]. 杭州: 浙江大学, 2017.

[36] Cui J L. Research on carbon nanotubes interconnect during the melting process of the solder using laser irradiating AFM probe[D]. Harbin: Harbin Institute of Technology, 2014.
崔健磊. 激光复合 AFM 探针热熔钎料的碳纳米管互连基础研究[D]. 哈尔滨: 哈尔滨工业大学, 2014.

[37] Cui J L, Zhang J W, Barayavuga T, et al. Nanofabrication with the thermal AFM metallic tip irradiated by continuous laser[J]. Integrated Ferroelectrics, 2017, 179(1): 140-147.

[38] Cui J L, Yang L J, Wang Y. Simulation study of near-field enhancement on a laser-irradiated AFM metal probe[J]. Laser Physics, 2013, 23(7): 076003.

[39] Lu X W, Yang L J, Xie H, et al. Simulations of the near-field enhancement on AFM tip irradiated by annular laser beam[J]. IEEE Transactions on Nanotechnology, 2019, 18: 979-982.

[40] Theogene B, Cui J L, Wang X W, et al. 3-D finite element calculation of electric field enhancement for nanostructures fabrication mechanism on silicon surface with AFM tip induced local anodic oxidation[J]. Integrated Ferroelectrics, 2018, 190(1): 129-141.

[41] Wang M S, Wang J Y, Chen Q, et al. Fabrication and electrical and mechanical properties of carbon nanotube interconnections[J]. Advanced Functional Materials, 2005, 15(11): 1825-1831.

[42] Xie B H, Fu W B, Fei G T, et al. Preparation and enhanced infrared response properties of ordered W-doped VO_2 nanowire array[J]. Applied Surface Science, 2018, 436: 1061-1066.

[43] Yin J F, Huang Y X, Hameed S, et al. Large scale assembly of nanomaterials: mechanisms and applications[J]. Nanoscale, 2020, 12(34): 17571-17589.

[44] Zheng F Z, Yang X, Wu Y, et al. Large-scale directed assembly of single-walled carbon nanotube devices by alternating current coupling dielectrophoresis[J]. Carbon, 2017, 124: 693-699.

[45] Chen C. Low dimensional nanomaterrials assemblies based on dielectrophoresis technology[D]. Harbin: Harbin Institute of Technology, 2012.
陈晨. 基于介电电泳技术的低维纳米材料组装[D]. 哈尔滨: 哈尔滨工业大学, 2012.

[46] Kalsin A M, Fialkowski M, Paszewski M, et al. Electrostatic self-assembly of binary nanoparticle crystals with a diamond-like lattice[J]. Science, 2006, 312(5772): 420-424.

[47] Lindgren E B, Derbenev I N, Khachatourian A, et al. Electrostatic self-assembly: understanding the significance of the solvent[J]. Journal of Chemical Theory and Computation, 2018, 14(2): 905-915.

[48] Walker D A, Kowalczyk B, de la Cruz M O, et al. Electrostatics at the nanoscale[J]. Nanoscale, 2011, 3(4): 1316-1344.

[49] Tang Z, Zhang Z, Wang Y, et al. Self-assembly of CdTe nanocrystals into free-floating sheets[J]. Science, 2006, 314(5797): 274-278.

[50] Yang P, Kim F. Langmuir-Blodgett assembly of one-dimensional nanostructures[J]. Chemphyschem, 2002, 3(6): 503-506.

[51] Collier C P, Saykally R J, Shiang J J, et al. Reversible tuning of silver quantum dot monolayers through the metal-insulator transition[J]. Science, 1997, 277(5334): 1978-1981.

[52] García Núñez C, Braña A F, López N, et al. Single GaAs nanowire based photodetector fabricated by dielectrophoresis[J]. Nanotechnology, 2020, 31(22): 225604.

[53] Singh S K, Aryaan N, Shikder M R A, et al. A 3D nanoelectrokinetic model for predictive assembly of nanowire arrays using floating electrode dielectrophoresis[J]. Nanotechnology, 2019, 30(2): 025301.

[54] Long J, Xiong W, Wei C, et al. Directional assembly of ZnO nanowires via three-dimensional laser direct writing[J]. Nano Letters, 2020, 20(7): 5159-5166.

[55] Song X H. Study on mechanism of carbon nanotube/metal interfacial bonding and related technology[D]. Shanghai: Shanghai Jiaotong University, 2010.
宋晓辉. 碳纳米管/金属界面键合机制及其相关技术

研究[D]. 上海: 上海交通大学, 2010.

[56] González-Rubio G, González-Izquierdo J, Bañares L, et al. Femtosecond laser-controlled tip-to-tip assembly and welding of gold nanorods[J]. Nano Letters, 2015, 15(12): 8282-8288.

[57] Son M, Jeong S, Jang D J. Laser-induced nanowelding of linearly assembled and silica-coated gold nanorods to fabricate Au @ SiO_2 core-shell nanowires[J]. The Journal of Physical Chemistry C, 2014, 118(11): 5961-5967.

[58] Bradshaw D S, Andrews D L. Manipulating particles with light: radiation and gradient forces [J]. European Journal of Physics, 2017, 38(3): 034008.

[59] Zhu C J, Song W Z, Qu M, et al. Thermal analysis and trapping properties of silicon-based optical nanotweezer structures [J]. Acta Optica Sinica, 2019, 39(3): 0324002.
朱晨俊, 宋五洲, 屈铭, 等. 硅基纳米光镊结构的热分析和捕获特性[J]. 光学学报, 2019, 39(3): 0324002.

[60] Min C J, Yuan Y Q, Zhang Y Q, et al. The hand of light for micro/nano-particle manipulation: research progress of optical tweezers[J]. Journal of Shenzhen University (Science and Engineering), 2020, 37(5): 441-458.
闵长俊, 袁运琪, 张聿全, 等. 操纵微纳颗粒的"光之手": 光镊技术研究进展[J]. 深圳大学学报(理工版), 2020, 37(5): 441-458.

[61] Pauzauskie P J, Radenovic A, Trepagnier E, et al. Optical trapping and integration of semiconductor nanowire assemblies in water[J]. Nature Materials, 2006, 5(2): 97-101.

[62] Song M X, Dellinger J, Demichel O, et al. Selective excitation of surface plasmon modes propagating in Ag nanowires[J]. Optics Express, 2017, 25(8): 9138-9149.

[63] Yang X G, Li B J. Localized and propagated surface plasmons in metal nanoparticles and nanowires[EB/OL]. (2018-11-05)[2020-11-15]. https://www.researchgate.net/publication/328913457_Localized_and_Propagated_Surface_Plasmons_in_Metal_Nanoparticles_and_Nanowires.

[64] Dufresne E R, Grier D G. Optical tweezer arrays and optical substrates created with diffractive optics[J]. Review of Scientific Instruments, 1998, 69(5): 1974-1977.

[65] Agarwal R, Ladavac K, Roichman Y, et al. Manipulation and assembly of nanowires with holographic optical traps[J]. Optics Express, 2005, 13(22): 8906-8912.

[66] Chen J, Ng J, Lin Z F, et al. Optical pulling force [J]. Nature Photonics, 2011, 5(9): 531-534.

[67] Yan Z J, Pelton M, Vigderman L, et al. Why single-beam optical tweezers trap gold nanowires in three dimensions[J]. ACS Nano, 2013, 7(10): 8794-8800.

[68] Wan H, Gui C Q, Chen D, et al. Scattering force and heating effect in laser-induced plasmonic welding of silver nanowire junctions [J]. Applied Optics, 2020, 59(7): 2186-2191.

[69] Crane M J, Pandres E P, Davis E J, et al. Optically oriented attachment of nanoscale metal-semiconductor heterostructures in organic solvents via photonic nanosoldering[J]. Nature Communications, 2019, 10(1): 4942.

[70] Min C J, Zhang Y Q, Zhang L C, et al. Plasmonic hybridization induced trapping and manipulation of metallic nano-objects [C]// Optoelectronic Devices and Integration 2015, June 16 - 19, 2015, Wuhan, China. Washington, D.C.: OSA, 2015: OW2B.3.

[71] Zhang L, Dou X, Min C, et al. In-plane trapping and manipulation of ZnO nanowires by a hybrid plasmonic field[J]. Nanoscale, 2016, 8(18): 9756-9763.

[72] Kotsifaki D G, Chormaic S N. Plasmonic optical tweezers based on nanostructures: fundamentals, advances and prospects[J]. Nanophotonics, 2019, 8(7): 1227-1245.

[73] Zhang Y, Shi W, Shen Z, et al. A plasmonic spanner for metal particle manipulation [J]. Scientific Reports, 2015, 5: 15446.

Progress of Pose Regulation and Laser-Induced Nanojoining Technique of One-dimensional Nanomaterials

Wan Hui[1], Zhao Qiang[1], Yu Shengtao[2], Luan Shiyi[2], Gui Chengqun[1*], Zhou Shengjun[1,2**]

[1] *The Institute of Technological Sciences, Wuhan University, Wuhan, Hubei* 430072, *China*;

[2] *School of Power and Mechanical Engineering, Wuhan University, Wuhan, Hubei* 430072, *China*

Abstract

Significance Due to the unique mechanical, electrical, thermal and optical properties, one-dimensional nanomaterials have a wide range of applications in micro- and nano- electro-mechanical systems, flexible transparent conductive devices, and sensors. Different from zero-dimensional and two-dimensional nanomaterials, one-dimensional nanomaterials have larger ratios of length to diameter. To build nano-structures or nano-devices with one-dimensional nanomaterials, both the position and posture (or rotation angle) need to be considered. Therefore, how to precisely control the pose of one-dimensional nanomaterials and then connect them with nanoscale, microscale, or bulk materials is crucial to realize the functionalization and deviceization of nanostructures.

Although one-dimensional nanomaterials have a variety of applications, precise manipulation of their pose and forming a reliable nanoscale interconnection with other materials are still great challenges. It is well known that nanomaterials have a small size, which makes them difficult to manipulate their poses. Manipulation methods, such as mechanical clamping, can easily cause damage to nanomaterials. In addition, the small size of nanomaterials results in a large specific surface area and high surface energy, which significantly reduces the melting point of nanomaterials and makes the nanomaterials susceptible to oxidation. How to connect nanomaterials and other materials without affecting the non-connection parts of nanomaterials is crucial for preparing high-performance nano-joints. To connect nanomaterials, many methods have been proposed, including mechanical pressing, thermal annealing, chemical treatment, cold welding, and light-induced plasmonic nanojoining. One of the potential nanojoining technologies is light-induced plasmonic nanojoining, which utilizes white light or laser to excite local surface plasmon resonances, thereby resulting in local heating. By precisely adjusting the intensity of the incident laser, the connection position of nanomaterials can be slightly melted, resulting in nanojoining of nanomaterial with other materials. Light-induced plasmonic nanojoining is a high-efficiency and low-damage nanojoining method.

In the past few years, various methods have been developed to manipulate the pose of one-dimensional nanomaterials, and then to join them by laser. According to the principle of nano-manipulation, these nano-manipulation methods are summarized into three types: probe method, self-assembly, and optical tweezers. Combining the pose manipulation with laser-induced plasmonic nanojoining of one-dimensional nanomaterials, we introduce the principles and characteristics of pose regulation of one-dimensional nanomaterials in detail, as well as the new development in laser-induced plasmonic nanojoining.

Progress The probe method utilizes probes to move and rotate one-dimensional nanomaterials to adjust their poses precisely. Due to the small size of one-dimensional nanomaterials, the probe tip is generally on the nanoscale. In addition, to manipulate the poses of one-dimensional nanomaterials, the probe method usually requires high-resolution microscope to locate nanomaterials. The microscopes used in the probe method include optical microscope (Fig. 1), atomic force microscope (Fig. 3), and scanning electron microscope (Fig. 4), and these probes include nano-fiber probes, atomic force microscope probes, and nano-tungsten needles.

Joining larger-scale one-dimensional nanomaterials is one of the keys for the realization of deviceization. A potential manipulation method is self-assembly. According to the principle of self-assembly of nanomaterials, there are three types of self-assembly methods. First, nanomaterials are subject to gravitational or repulsive force in solutions, and then self-assembly is realized under dynamic equilibrium. Second, nanomaterials are self-assembled through the Langmuir-Blodgett technology by the surface tension of liquid-gas or solid-liquid interfaces. Third, under the action of external fields, such as electric field, magnetic field, and light field (Fig. 6), the polarized nanomaterials are moved along the gradient direction, and the moving direction of polarized nanomaterials is determined by the relative permittivity of the solution and the nanomaterials (Fig. 5).

To further improve the precision and efficiency of nano-operation, optical tweezers are used to manipulate the

poses of one-dimensional nanomaterials. Single-beam optical tweezer has been used to manipulate the poses of semiconductor nanowires (Fig. 7). To improve the stability of nano-manipulation, holographic optical tweezers or optical tweezer arrays are used for nano-manipulation (Fig. 8). Photons have momentum. The exchange of momentum between photons and nanomaterials produces scattering forces. Unless the gradient force generated by the optical tweezers can overcome the scattering force acting on nanomaterials, or the nanomaterials are pushed away by the scattering force. For wide-bandgap semiconductor materials, infrared lasers can pass through one-dimensional nanomaterials. Therefore, the scattering force acting on one-dimensional nanomaterials is very weak. But for metal nanomaterials, the scattering force acting on them increases significantly due to their good conductivity. As a result, it is difficult to use conventional optical tweezers to manipulate the poses of one-dimensional metal nanomaterials. To manipulate the poses of metal nanomaterials, plasma tweezers are developed (Fig. 9).

Conclusions and Prospects According to the characteristics of the aforementioned nano-manipulation technology, it is observed that the probe technology can be used to manipulate the pose of one-dimensional nanomaterials, to test the conductivity and reliability of the laser-prepared nanostructures. However, the probe technology has a low efficiency of nano-manipulation efficiency. Self-assembly technology has unique advantages in the larger-scale operation of one-dimensional nanomaterials, but the commonly used dielectrophoresis methods need to be performed under a specific electrode structure, and the precision of nano-manipulation is relatively low. Optical tweezer technology has high nano-operation accuracy. The laser source can be used for nano-operation and nanojoining, but it needs to be carried out in solutions. These problems indicate that improving the compatibility of self-assembly and optical tweezer technology with the existing microelectronic processes is the focus of future research. Based on the above research results, we believe that multi-technology integration is the future development trend. It is found that nano-manipulation technology is merging with laser, microscopy, and nano-testing technology to realize nano-observation, nano-operation, nano-joining, and nano-testing. This kind of multi-functional technology and equipment will further promote the development and application of nano-technology, promote multi-disciplinary cross, and produce more innovative applications.

Key words laser technology; laser-induced nanojoining; one-dimensional nanomaterials; pose regulation

OCIS codes 140.3390; 160.4236; 230.4000